Early-age heat evolution of clinker cements in relation to microstructure and composition: implications for temperature development in large concrete elements

Y. Ballim *, P.C. Graham

School of Civil and Environmental Engineering, University of the Witwatersrand, Private Bag 3, WITS, 2050 Johannesburg, South Africa

Abstract

This paper presents an assessment of the range and extent of variation of heat evolution of nominally similar cement clinkers from a range of cement production facilities in South Africa. Clinker samples were collected at nine cement plants and cements were prepared by grinding each clinker with a uniform quality of gypsum. X-ray fluorescence and optical microscope techniques were then used to characterise each clinker and cement in terms of chemical composition and cement compound morphology.

Concretes were then prepared with the laboratory-manufactured cements and these were tested in an adiabatic calorimeter in order to determine the rate of heat evolution from each of the clinker samples. The results of these tests were related to the chemical and morphological characteristics of the corresponding cement clinkers. The results indicate a clear differentiation of clinker cements into low, medium and high heat cements. The relationships between this classification of the heat performance of the cements and the chemistry and morphology of the clinker is not clear at this stage. However, using a finite difference heat model, the paper presents an indication of the implications of the measured heat characteristics of the cement for early-age temperature distributions in large concrete elements.
© 2003 Elsevier Ltd. All rights reserved.

Keywords: Cement; Clinker; Chemistry; Morphology; Fineness; Heat; Microscopy; Modelling; Mass concrete

1. Introduction

The thermal response of concrete due to hydration of cement is a predominant factor in the potential for early-age cracking of large concrete elements. An analysis of this cracking potential requires an ability to quantify both the amount of heat that is evolved by the cement as well as the rate at which this heat is evolved [1]. Both these parameters are strongly influenced by the chemical and mineralogical composition of the cement, insofar as it affects the kinetics of the hydration reactions of cement. Furthermore, clinker morphology has been shown [2] to influence the compressive strength and, by inference, the hydration development of cement. Clearly, an ability to estimate the thermal response of cement in concrete, based on a knowledge of clinker characteristics would be of assistance to mass concrete

designers and cement manufacturers seeking to control temperature development in such structures.

The kinetics of Portland cement hydration and associated rates of heat evolution have been commented on by a number of authors [3–8]. Earlier work [3–6] favoured the view that the total heat liberated by a cement is the mass weighted sum of the heat liberated by the individual pure crystallographic components. In this regard, Copeland et al. [5] comment that "the contribution of each component of a completely hydrated cement paste is, within experimental error, the heat of hydration of the pure components". However, later work by van Breugel [7] and Kishi et al. [8] argues that the concept of independent hydration of the clinker components requires correction to account for interaction between the cement components during hydration. This concept of component interaction during hydration has been adopted in much of the numerical models developed to simulate the hydration process and associated heat evolution [7–9].

The research reported in this paper was undertaken to quantify the range and extent of variation in the rates of

---

* Corresponding author. Fax: +27-11-339-1762.
E-mail address: ballim@civil.wits.ac.za (Y. Ballim).

heat evolution of nominally similar cement clinkers in South Africa. As a secondary objective, the research was aimed at assessing if the observed variations in heat evolution characteristics can be explained by differences in clinker chemistry and mineralogy, based on chemical and microscopic evaluation of the clinkers. Finally, the objective was to assess the effects of variations in the heat evolution characteristics of South African cements on the early-age temperature development in typical mass concrete structures placed under controlled conditions.

Nine clinker samples were obtained from different manufacturing facilities in the country. A cement was produced from each clinker by grinding with a controlled amount of the same gypsum. The chemical composition of the clinkers and the gypsum were determined using X-ray fluorescence (XRF) and samples of the raw clinkers were mounted, polished and etched for optical microscope study. These results were then used to characterise the crystallographic and chemical properties of the cements.

Each cement was used to prepare a concrete with fixed mixture proportions and aggregate type. The concretes were tested in an adiabatic calorimeter in order to determine the rate and amount of heat evolved by the cements. Comparisons of the heat of the heat properties of the different cements were made on the basis of a maturity function rather than clock time.

The results of the adiabatic tests were also used to indicate the implications of the different heat characteristics of cements for the time–temperature profiles in a large, high strength beam element and a low strength mass concrete element. A finite difference heat flow model was used in this analysis.

2. Clinker sampling and preparation

2.1. Sample collection

Cement clinker samples were drawn from nine production plants belonging to three cement companies operating in South Africa. Each of these production plants manufacture Type 1 cement which satisfies the requirements of the local standard specification, SABS ENV 197 [10]. To ensure that the samples were representative of current production, the clinker was drawn from the moving stock just before entry into the grinding mill. Approximately 4 kg of clinker was drawn from each plant and 500 g of each sample was reserved for microscopy and chemical analysis. The remaining 3.5 kg was used to manufacture cement in the laboratory.

2.2. Gypsum for cement manufacture

In order to manufacture the cements in the laboratory, a sample of gypsum was obtained from one of the

Table 1
Chemical composition of the gypsum used in the cements and the amount of gypsum added to each clinker

	% by mass	Clinker identification	% Gypsum added (by mass)
CaO	30.20	A	3.683
SiO_2	6.90	B	4.910
Fe_2O_3	0.44	C	5.031
Al_2O_3	0.60	D	5.010
MgO	0.80	E	5.147
TiO_2	0.04	F	4.490
Mn_2O_3	0.02	G	4.984
K_2O	0.19	H	5.120
Na_2O	0.25	K	4.490
SO_3	41.00		
P_2O_5	0.00		
LOI	18.25		

production plants and, based on a chemical analysis of the gypsum and the clinkers, the amount of gypsum added to each of the clinkers was adjusted so that each cement had an SO_3 content of 2.3%. The same gypsum type and SO_3 content was used to ensure that the rate of heat evolution of each clinker was compared on the basis of clinker characteristics only. Also, while an SO_3 content of 2.3% is typical of South African cements, in reality, manufacturers would adjust the SO_3 content in response to variations in aspects such as the C_3A content of the clinker. Table 1 shows the chemical composition of the gypsum used, based on an XRF analysis, as well as the proportion of gypsum added to each of the cement clinkers.

2.3. Grinding and cement fineness

Each clinker with the appropriate amount of gypsum was ground in a laboratory ball mill. The mill was periodically stopped and the specific area of the sample was determined using the Blaine test [11]. Grinding was stopped when the measured specific surface area of the sample was 3200 ± 50 cm²/g. Using this procedure, the average fineness measured for the nine samples was 3198 cm²/g with a standard deviation of 24 cm²/g.

3. Test methods

3.1. X-ray fluorescence

XRF was used to determine the chemical compound composition of the clinkers. The analyses were conducted using ground clinker samples and these results were also used to determine the required amount of gypsum for each cement. This analysis was conducted in the laboratory of one of the cement producers, where XRF is used for routine quality control purposes. The instrument is regularly calibrated and checked for operational accuracy. The samples used in this project were

placed in the automatic feed system of the instrument alongside the routine production sample analyses.

3.2. Optical microscopy

A geological polarising microscope with reflected light capability, was used to assess the structure and morphology of polished and etched samples of each of the clinkers. The clinker samples were lightly crushed using a steel pestle and the −2.36 to +1.18 mm fraction was used to prepare the polished sections. The fragments were encapsulated in epoxy and one surface was polished, initially with 600 grit carborundum paper, followed by progressively finer abrasion systems, until a final polish with 0.25 μm diamond paste, on a lapping disk with a non-aqueous lubricant.

The polished samples were then etched using a procedure recommended by St John et al. [12]. This procedure involves the following treatment of the polished surface of the sample:

- 20 s immersion in a 10% solution of KOH in ethyl alcohol to etch the C_3A and C_4AF phases;
- rinse in ethyl alcohol;
- brief rinse in isopropyl alcohol and light buff with paper towel;
- 6 s immersion in a solution of 1.5 ml HNO_3 in 100 ml isopropyl alcohol to etch mainly the alite (C_3S) and the belite (C_2S) phases;
- rinse in isopropyl alcohol.

Digital photo-micrographs were then obtained of the etched surfaces and an image analysis system was used to measure crystal sizes and to provide a qualitative description of the clinker morphology.

3.3. Adiabatic calorimetery

3.3.1. Expressions for the rate of heat evolution

The adiabatic calorimeter proposed by Gibbon et al. [13] was used to determine the amount and rate of heat evolved by each of the laboratory cement samples. In essence, the calorimeter uses a 1 litre sample of concrete in a bath of water but separated from direct contact with the water by a 40 mm thick air space. A temperature probe in the concrete sample is monitored by a personal computer fitted with an analogue-to-digital input/output card. A heater element in the water bath is then turned on or off in response to the concrete temperature to maintain the water bath at the same temperature as that of the concrete. The concrete temperature is then monitored over time and the amount of heat per unit mass of cement (q_t) is determined from:

$$q_t = C_p \cdot (T_t - T_0) \cdot \frac{m_s}{m_c} \tag{1}$$

where C_p is the specific heat capacity of the concrete, determined as the mass weighted average of the specific heat capacities of the concrete components and, as discussed by Gibbon et al. [13], is assumed to be constant throughout the test; T_t is the temperature of the concrete sample at time t during the adiabatic test and T_0 is the sample temperature at the beginning of the test; m_s is the mass of the concrete test sample and m_c is the mass of cementitious binder in the sample.

The heat rate ($\dot{q}_t$) is conventionally determined by differentiating Eq. (1) with respect to time, so that:

$$\dot{q}_t = \frac{dq_t}{dt} \tag{2}$$

The time basis of Eq. (2) presents a problem because of the circular relationship between the rate of heat evolution, the extent of hydration, time and the temperature at which the hydration reactions take place. This is generally addressed by expressing the heat rate (as in Eq. (2)) as a function of maturity [7,14], rather than time. Hence, the heat rate applicable to a particular point in a structure at a given time is determined by the maturity (or time–temperature history) at that point. Stated differently, at a given point in time, the heat rate will vary across a concrete section in accordance with the variation in maturity across the section.

In order to normalise the heat curves to an equivalent degree of advance of hydration, the time axis is expressed in terms of Arrhenius maturity development [15], which, in its relative form, is written as:

$$t_{20} = \sum_{i=1}^{i=n} \exp\left[\left(\frac{E}{R}\right) \left(\frac{1}{293} - \frac{1}{273 + 0.5 \cdot (T_i + T_{i-1})} \right) \right] \cdot (t_i - t_{i-1}) \tag{3}$$

The reference temperature in Eq. (3) is taken as 20 °C and t_{20} is the equivalent maturity time (in h); E is the activation energy parameter (33.5 kJ/mol, taken as constant [16]); R is the universal gas constant (8.314 J/mol °C); T_i is the temperature (°C) at the end of the ith time interval, t_i.

Noting that the rate of hydration and therefore, the rate of heat evolution, is dependent on the absolute temperature, Ballim and Graham [17] have shown that, since Eq. (1) accounts only for temperature differences, the rate of heat evolution determined from an adiabatic calorimeter test should be normalised with respect to maturity, rather than time. This means that, rather than the form shown in Eq. (2), the heat rate should be expressed as:

$$\dot{q}_M = \frac{dq_t}{dM} \tag{4}$$

Expressing the maturity heat rate (Eq. (4)) as a function of the cumulative maturity, allows the heat rate curve to be normalised so as to be independent of the starting temperatures in the adiabatic test.

It should be noted that normalising the heat rate curves using a maturity function as described above, effectively converts the adiabatic heat rate curve to an equivalent isothermal calorimetery curve. With this approach, an error may be introduced by assuming a constant value for the activation energy parameter (E). Broda et al. [18] have shown that E varies with temperature during hydration but note that the variation is fairly small and that a single value would suffice. In an assessment of blended cements using isothermal calorimetry, Xiong and van Breugel [19] show similar variations in the apparent activation energy with the progress of hydration. However, they also conclude that this variation "…may be less important in real engineering practice…".

3.3.2. Sample preparation and testing

The nine laboratory cements were each used to make a concrete sample with the mixture composition as shown in Table 2. All the mixture components, including the water, were stored in the same room as the cal-

Table 2
Mixture composition of the concrete used for the adiabatic calorimeter tests

Laboratory cement	350 kg/m³
9.5 mm washed silica stone	850 kg/m³
Graded, washed silica sand	885 kg/m³
Water	233 l/m³

orimeter at least 24 h before mixing. This allowed the temperature of the materials to equilibrate to the room temperature, which was controlled at 19 ± 1 °C. A 1.2 l sample of each concrete was prepared by manual mixing in a steel bowl and the adiabatic test was started within 15 min after the water was added to the mixture. All the tests were started at temperatures between 18 and 20 °C and temperature measurement in the calorimeter was continued for approximately four days.

The silica sand used in the concretes was obtained in four size fractions and these were recombined as needed for the mixing operation to ensure a uniform sand grading for each concrete.

4. Results and discussion

4.1. XRF analysis

Table 3 shows the results of the XRF analyses of each of the clinker samples. The table also shows the calculated proportions of the four main cement mineral phases in each clinker based on the Bogue analysis [20]. It was not thought necessary to apply the modifications to the Bogue analysis as proposed by Taylor [21] since the analysis was conducted on clinker samples. In this case, the error incurred in the analysis would not be significantly improved for rapidly cooled clinkers such as those tested in this investigation. Table 3 also shows

Table 3
Results of XRF analysis of the clinker samples and Bogue calculation of crystalline phase composition

	A	B	C	D	E	F	G	H	K
% Composition of clinker									
CaO	66.50	68.16	66.50	65.57	68.40	67.60	67.60	65.06	65.6
SiO$_2$	22.30	23.03	21.20	22.15	22.10	22.20	22.80	22.26	21.90
Fe$_2$O$_3$	3.61	2.28	3.03	2.98	4.26	3.33	1.90	3.05	1.57
Al$_2$O$_3$	3.80	3.82	4.20	4.51	3.80	4.40	4.30	3.98	5.00
MgO	1.10	1.48	3.30	2.64	0.50	0.80	1.40	2.04	3.70
TiO$_2$	0.18	0.31	0.30	0.45	0.19	0.21	0.28	0.25	0.26
Mn$_2$O$_3$	0.05	0.17	0.61	0.22	0.09	0.06	0.24	0.99	0.72
K$_2$O	0.62	0.13	0.25	0.16	0.39	0.57	0.58	0.53	0.32
Na$_2$O	0.37	0.00	0.12	0.20	0.19	0.18	0.06	0.14	0.11
SO$_3$	0.82	0.30	0.25	0.26	0.20	0.48	0.27	0.21	0.48
P$_2$O$_5$	0.15	0.00	0.02	0.00	0.16	0.13	0.03	0.00	0.10
Free lime	1.02	1.10	1.25	0.80	0.82	0.61	1.57	0.97	0.35
LOI	0.80	0.30	0.58	0.00	0.64	0.12	0.98	0.90	0.16
Total	100.20	99.98	100.30	99.14	100.80	100.80	100.40	99.41	99.92
Alumina ratio	1.05	1.67	1.39	1.51	0.89	1.32	2.25	1.31	3.16
Silica ratio	3.03	3.80	2.96	2.98	2.77	2.90	3.70	3.19	3.36
Crystalline phase composition (%) of clinker by Bogue analysis									
C$_3$S	66	69	72	61	75	70	64	61	63
C$_2$S	14	14	7	18	6	11	17	18	15
C$_3$A	4	6	6	7	3	6	8	5	11
C$_4$AF	11	7	9	9	13	10	6	9	5

the calculated values of the alumina and silica ratios as defined in Ref. [12].

The following points are noted from the results presented in Table 3:

- The chemical compound analysis of the clinkers generally lie within the limits proposed by Addis [22] for South African cements. This means that the nine clinker samples selected can be considered typical of South African clinkers intended for cement manufacture.
- Clinker E shows an unusually high content of Fe_2O_3 which explains the high calculated C_4AF content of this clinker.
- Clinker K is unusual in the group because of the significantly higher MgO (periclase) content as well as the higher Al_2O_3 content.
- Accepting that the Bogue analysis indicates likely or potential compound development, the results indicate that the higher alite content of clinkers B, C, E and F is likely to result in relatively high early-age heat results because of the strong influence of this compound on heat liberation during early hydration [21].
- The relatively high C_3A content of clinker K is also likely to add significantly to the early heat evolution of this clinker.
- Considering the alkali content of the cement (K_2O and Na_2O), clinker B is particularly low in alkali content, with these values falling below the minimum value suggested by Addis [22] for South African cements (range 0.2–0.8%).

4.2. Optical microscopy

Fig. 1 shows sample photo-micrographs of some of the clinkers viewed under reflected light after etching. In general, the C_3S crystals appear large and angular to subangular, while the C_2S crystals are smaller, rounded and often striated. The interstitial material between these crystals is mainly composed of C_4AF and C_3A. Table 4 presents a summary of the observations made during the microscopic assessment of the clinker. Note that, in this table, the term "dendritic" is used in its geological sense to mean a "tree-like" distribution of crystal growth, forming a cluster of small crystal nodules which are poorly connected to each other.

4.3. Adiabatic calorimetry

Fig. 2 shows the results of the adiabatic calorimeter tests conducted with the concretes containing each of the laboratory cements. The results are presented as the total heat liberated by the cement (per unit mass), as calculated using Eq. (1). The specific heat (C_p) was taken as the mass weighted average of the concrete mixture components (as shown in Table 2) and was calculated to
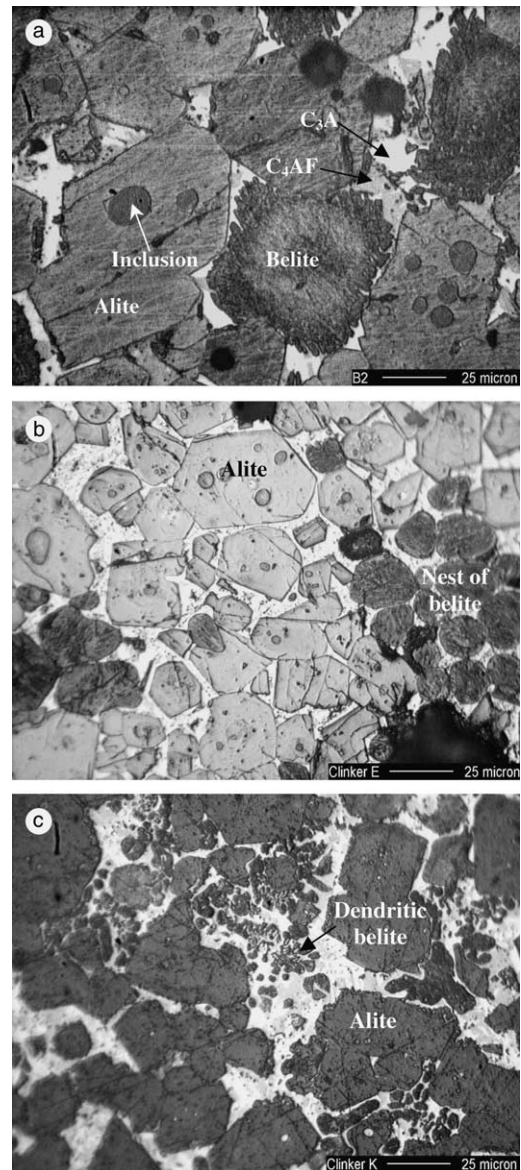

Fig. 1. Sample photo-micrographs of the clinkers showing: (a) ragged edges of C_2S—clinker B; (b) nests of C_2S—clinker E; (c) Dendritic distribution of C_2S—clinker K.

be 1270 J/kg K. The time axis is presented as equivalent maturity hours, determined using the Arrhenius function shown in Eq. (3). There is clearly strong overlap of many of the curves and only those curves which are separately identifiable have the corresponding clinker cement indicated on Fig. 2.

The adiabatic test was terminated when the sample showed no appreciable increase in temperature. This is the point at which the rate of hydration of the cement is so slow that the heat being evolved is not sufficient to increase the temperature of the sample to a level that is measurable by the temperature probes. For most of the cements tested, this point was reached before 600 maturity hours. However, in the case of clinker cement E,

Table 4
Summary of observations made during the microscopic examination of the clinker samples

| Clinker	C_3S	C_2S	Interstitial phase
A	Angular, euhedral crystal shape, generally hexagonal; crystal size from 20 to 60 μm	Well distributed with occasional nests; rounded, oval or pear-shaped crystals; crystal size in the range 15–55 μm	Generally thinly distributed, especially in areas where C_3S and C_2S are tightly packed
B	Angular, euhedral crystal shape, generally hexagonal; crystal size from 20 to 60 μm; most crystals have C_2S inclusions	Well distributed with occasional nests; rounded shapes with ragged edges; crystal size in the range 20–50 μm	Well distributed matrix with approximately equal aluminate and ferrite phases
C	Dominant crystal form; many crystals have joined but retain the angular structure; crystal size from 10 to 50 μm	Sparse distribution; individual crystals rare and mainly occurs as flows between the C_3S crystals; crystal size from 3 to 15 μm	Well distributed matrix; aluminate clearly discernable and appears as localised patches or concentrated spots
D	Crystals usually angular with common pseudohexagonal shapes; crystal size from 10 to 50 μm; some large inclusions	Well distributed in small nests; rounded, oval or pear-shaped crystals; crystal size in range 10–30 μm; narrow rims on C_3S crystal edges	Well distributed throughout; poor distinction between phases; aluminates appear present as localised patches
E	Dominant crystal form; angular with pseudohexagonal shapes; crystal size from 10 to 55 μm; C_2S inclusions common	Well distributed in small nests; rounded to oval-shaped crystals; crystal size in range 10–35 μm; distinct lamellar structure	Good distribution with occasional abutting C_3S grains; aluminate in the form of narrow streaks—possibly dendritic
F	Tightly packed with much joining while retaining angular shape; small inclusions which are not common	Well distributed in small nests; rounded to oval-shaped crystals; crystal size in range 20–30 μm; distinct lamellar structure	Good distribution; aluminate in the form of small patches and narrow streaks—possibly dendritic
G	Relatively small grains: 5–35 μm; angular with pseudohexagonal shapes; inclusions common	Rounded to oval; small crystals: 5–40 μm; thin zones on edges of C_3S	Aluminate phase prevalent; large patches with small ferrite areas
H	Tightly packed grains; joined to form subhedral shapes; 10–50 μm; some inclusions	Well distributed in small and large nests; rounded to pear shaped; 10–30 μm	Aluminate phase in dendritic form
K	Crystals angular euhedral; often joined; 10 to 40 μm; inclusions small and rare	Individual crystals rare; generally occurs in the matrix in dendritic crystals or as rims on C_3S grains	Well distributed and rich in aluminate; small amounts of periclase visible
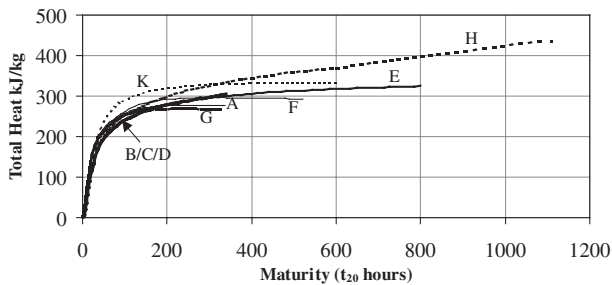
Fig. 2. Heat curves determined from the adiabatic tests for the nine clinker cements tested.

Fig. 3. Heat rate curves for the cements tested in the adiabatic calorimeter.

this point was only reached at approximately 800 maturity hours and, in the case of clinker cement H, measurable temperature increases continued to be recorded after 1100 maturity hours. This trend was confirmed by re-testing of this cement. The reason for this behaviour are not clear at this stage and certainly require further investigation.

The results shown in Fig. 2 were converted to the maturity heat rate form using Eq. (4) and Fig. 3 shows the calculated heat rates for the nine cements in this form. The units of the heat rate in this figure are unconventional and are best described as ''maturity watts'' per kg of cement (J/maturity second/kg).
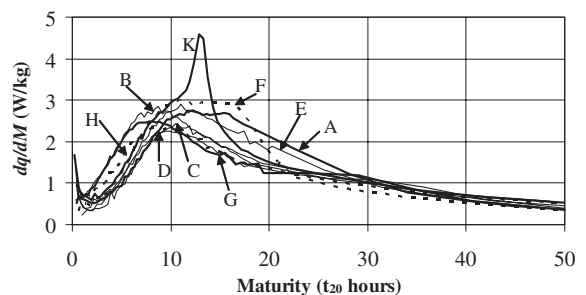
Fig. 3 again shows considerable overlap and only the clearly discernable curves are identified. Expressed in this form, clinker cement K stands out in the brief but significantly larger heat rate at between 15 and 20 maturity hours. To improve the clarity, the curves in Fig. 3 are shown only for the first 50 maturity hours. Beyond this point, the curves bunch together and individual characteristics are not discernable.

Based on the heat rate curves shown in Fig. 3, the clinker cements fall into three distinct groups in terms of the maximum heat rate as follows:

- high heat—clinker cement K;
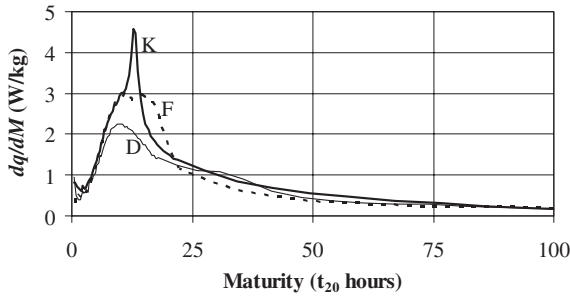- medium heat—clinker cements A, B, E, F and H;

Fig. 4. Three clinker cements representative of the three proposed heat rate groups.

- low heat—clinker cements C, D and G.

For clarity, representative curves of each of these three groups are extracted from Fig. 3 and shown in Fig. 4.

The essential difference between the three curves shown in Fig. 4 lies in rate of heat evolution between 10 and 25 maturity hours. Outside of this maturity range, the heat rates show only marginal differences. The average maximum measured heat rates for each of the three groups are 2.2 J/maturity second/kg for the low heat group, 3.0 J/maturity second/kg for the medium heat group and 4.6 J/maturity second/kg for clinker cement K. This indicates that the heat rate model proposed by Wang and Dilger [14] is only appropriate for the low heat group of clinker cements tested in this investigation. Their model sets a maximum heat rate of 2.2 W/kg occurring at 10 maturity hours.

4.4. Relating heat rates to physico-chemical characteristics of the clinker

Considering the results of the XRF analysis presented in Table 3, the qualitative description of the clinker morphology characteristics presented in Table 4 and the heat rate classifications presented above, the following points are noted:

- The high heat rate performance of clinker K seems to be related to the high C_3A content, which is also reflected in a high alumina ratio. While working with significantly different cements at the time, Lerch [23] noted similar "spikes" in the rate of heat evolution of cements with high C_3A contents. He also noted that the magnitude of the heat rate "spike" decreased and the time of its occurrence increased as the SO_3 content of the cement increased. Macphee and Lachowski [24] note that the presence of periclase has the effect of reducing the hydration kinetics of the cement. However, in the case of clinker K, it appears that the effect of the relatively high periclase content is overshadowed by the effect of the high C_3A content. Furthermore, given the finer distribution of the dendritic form of belite in this clinker, this phase

may show earlier hydration than would normally be expected with more typical belite phases. However, the extent to which this contributes to early heat evolution will require further investigation.

- There appears to be very few common chemical or morphological characteristics between clinkers A, B, E, F and H to indicate that they should belong in a joint heat rate category as measured in the adiabatic calorimeter tests. This is particularly so when considering the clinkers that have been categorised as low-heat clinkers (C, D and G). These two groups of clinker are not distinguishable on the basis of the chemical analysis or the morphological descriptions.
- Because of the relatively high alite contents, none of the clinkers assessed conform to the description of a "typical low-heat" cement as described by Jackson [25], who suggests a C_3S content of 34% for this cement classification.

At this stage, we should speculate that the characterisation techniques used for the clinkers has not provided sufficient information to discriminate between the clinkers on the basis of the rate of heat liberation. It may be that a more detailed analysis of the polymorph [26] composition of the clinker phases is necessary to better understand the hydration kinetics of a particular phase. A further useful analysis would be to consider the phase distribution in the different size fractions of the ground cement. Cements with a higher proportion of alite in the finer fractions can be expected to show higher rates of heat evolution, even if the bulk alite content is not unusually high.

4.5. Modelling the rate of heat evolution

The composition heat rate model developed by Maekawa et al. [27] was used to assess the ability of such a model to predict the heat rates of the cements tested in this study. The model was adjusted to express the heat rate in terms of maturity time (t_{20} h). Fig. 5 shows a comparison of the measured and predicted heat rates for
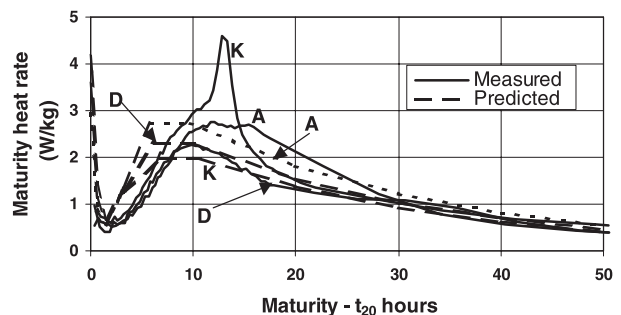

Fig. 5. Comparison between the measured and predicted heat rate curves for clinker cements A, D and K using the Maekawa et al. model [27].

clinkers A, D and K which indicate the range of typical results. In some cases, the prediction was particularly good (clinker D), while in others, the model predicted the peak heat rate correctly, but the timing of the peak was time-shifted from that measured. In the case of clinker K, the model showed particularly poor prediction. It therefore seems that the parameters accounted for in the model are not always sufficient to describe the heat evolution characteristics of clinker cements.

5. Effects of the measured heat rates on actual structures

Our interest in the rate of heat evolution of cement derives primarily from concern for the maximum temperatures likely to occur in concrete structures. The implications of the different heat rates for the cements assessed in this programme was therefore investigated using a modified version of the finite difference heat model proposed by Ballim [28]. The model was run using the three heat curves shown in Fig. 4 (D, F and K), representing the low, medium and high heat rate clinker cement groups. The intention here is not to try to reflect field conditions but rather to indicate the temperature effects of using the different cements in large concrete elements under controlled conditions. In reality, concrete for large structures would normally have significant proportions of cement extenders (fly ash or blastfurnace slag) and include admixtures to reduce the rate of heat evolution.

Two structures were assessed using the three heat rate curves as input into the model:

- A concrete block, typical of that used for dam wall construction, measuring 4 m wide and 3 m deep; cement content = 200 kg/m^3; concrete specific heat capacity = 1120 J/kg °C; concrete density = 2430 kg/m^3.
- A concrete beam measuring 500 mm square; cement content = 475 kg/m^3; concrete specific heat capacity = 1200 J/kg °C; concrete density = 2385 kg/m^3.
- The thermal conductivity of the concrete is 2.7 W/m °C as suggested by van Breugel [7] for granite aggregate concrete.

Furthermore, the external and processing conditions used in the modelling exercise for both structures, were as follows:

- the concrete is cast directly onto rock with a thermal conductivity of 1.2 W/m °C;
- concrete is placed at a temperature of 17 °C and the ambient temperature varies sinusoidally between 16 and 20 °C;
- the side formwork is held in place for 18 h after casting, during which time the heat transfer coefficient from these surfaces is taken as 5 W/m^2 °C;
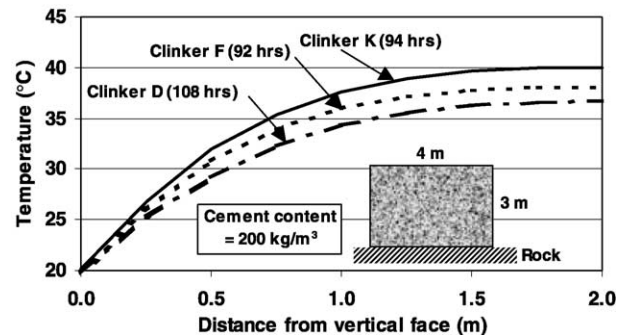

Fig. 6. Variation in the modelled temperature across a central section of a large concrete block at the time when the maximum temperature occurs, for the three cement heat rates assessed.

- upon removal of the formwork, the heat transfer coefficient for the side surfaces is taken as 25 W/m^2 °C, representing a surface directly exposed to a mild wind.

Fig. 6 shows the modelled temperatures for large concrete block from the vertical surface to the centre of the block, across a section 1.5 m below the top surface and at the time when the maximum internal temperature occurs. The time to reach the maximum temperature varied for the different clinker cements and this is indicated in Fig. 6 in parentheses alongside the clinker cement identification.

In this application, Fig. 6 shows that the higher the maximum heat rate of the binder as measured in the adiabatic calorimeter, the higher is the maximum temperature obtained on the structure. For the three clinker cements assessed, the maximum temperature varied from 40 °C for clinker cement K, 38 °C for clinker cement F and 36.5 °C for clinker cement D. Also, while the maximum temperature for clinker cements F and K occurred at approximately 93 h after casting, the maximum temperature was only reached at 108 h for clinker cement D. In addition to the lower temperature gradient that occurs with clinker cement D, the later occurrence of the maximum temperature may further mitigate the potential for cracking, assuming that the creep capacity remains relatively unchanged during this period.

Fig. 7 shows the modelled temperatures across the high strength beam from a vertical surface to the centre of the beam, across a section 250 mm below the top surface. The temperatures shown in Fig. 7 occur at 20 h after casting for each of the clinker cements assessed, which is when the maximum internal temperature occurs. In comparison with the results shown in Fig. 5 for the large concrete block, Fig. 7 shows that:

- there is very little difference between the effects of clinker cements F and K in the maximum temperature profile obtained in the beam—possibly because
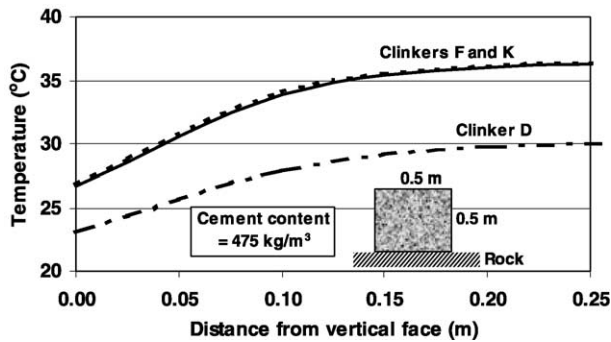
Fig. 7. Modelled temperatures across a central section of a concrete beam at the time when the maximum temperature occurs, for the three cement heat rates assessed.

the "spike" of high heat rate shown by clinker cement K is of too short a duration to have a significant effect in this application where heat dissipation is more rapid;

- on average, the three cements show temperature differences between the surface and the centre of the beam of approximately 8 °C, which is significantly smaller than the corresponding value of approximately 18 °C obtained for the concrete block;
- using clinker cement D to construct the beam (Fig. 7) results in a maximum temperature which is 6 °C lower than that obtained when using clinker cements F or K.

6. Conclusions

(1) Considering the maturity rate of heat evolution, the nine clinker cements tested can be categorised into high, medium and low heat cements based on the maximum measured heat rate. The average maximum heat rates obtained in each of these categories were: 2.2 J/maturity second/kg for the low heat group, 3.0 J/maturity second/kg for the medium heat group and 4.6 J/maturity second/kg for the high heat cement.

(2) Within this categorisation, only clinker cement K was placed in the high heat category, clinker cements A, B, E, F, and H were categorised as medium heat cements and clinker cements C, D and G were considered as low heat cements.

(3) XRF analysis for chemical composition and qualitative microscopy for morphological characterisation of cement clinker, in themselves, do not provide sufficient information to allow a heat-rate characterisation of the cement derived from such a clinker. It is suggested that this information should be combined with further analysis of the clinker involving a thorough characterisation of the crystallographic forms and an assessment of the phase distribution in different size fractions of the ground cement.

(4) Based on a finite difference heat model analysis, it appears that the categorisation of low, medium and high heat cements is more significant for the temperature development in low cement content, mass concrete structures than for high-strength, relatively small concrete elements. Importantly, the maturity duration of the measured peak heat rate of the cement is an important in determining the effect of maximum heat rate on temperature development in smaller concrete elements. For the present study, because of the relatively short duration of the peak heat rate of clinker cement K, the effect of the medium and high heat rate cements were almost identical when considering the temperature development in a 0.5 m thick concrete beam-type element.

References

[1] Hughes BP, Mahmood AT. Laboratory investigation of early age thermal cracking of concrete. ACI Mater J 1988;(May/June).

[2] Campbell DH. A summary of Ono's method for cement quality control with emphasis on belite color. In: de Hayes SM, Stark D, editors. Petrography of cementitious materials. ASTM STP 1205. Philadelphia: American Society for Testing Materials; 1994.

[3] Bogue RH. The chemistry of Portland cement. 2nd ed. New York: Reinhold Publishing Corporation; 1955.

[4] Bye GC. Portland cement—composition production and properties. Oxford: Pergamon Press; 1983.

[5] Copeland LE, Kantro DL, Verbeck G. Chemistry of hydration of Portland cement. In: 4th International Symposium on the Chemistry of Cement. US Department of Commerce, Washington, 1962.

[6] Steinhour HH. The reactions and thermochemistry of cement hydration at ordinary temperature. In: 3rd International Symposium on the Chemistry of Cement. Cement and Concrete Association, UK, 1952.

[7] vanBreugel K. Prediction of temperature development in hardening concrete. In: Springenschmid R, editor. Prevention of thermal cracking in concrete at early ages. London: E&FN Spon; 1998. p. 51–75. RILEM Report 15 [Chapter 4].

[8] Kishi T, Shimomura T, Maekawa K. Thermal crack control design of high performance concrete. In: Proceedings of the International Conference "Concrete 2000" Dundee, Scotland. London: E&FN Spon; 1993.

[9] Garboczi EJ, Bentz DP. Computer based models of the microstructure and properties of cement-based materials. In: Proceedings of the 9th International Conference on the Chemistry of Cement, vol. VI. New Delhi, 1992. p. 3–15.

[10] SABS ENV 197-1:2000. Cement—Part 1: Composition, specifications and conformity criteria for common cements. South African Bureau of Standards, Pretoria, 2000.

[11] SABS SM 748:1971. Standard test method: specific surface of cement. South African Bureau of Standards, Pretoria, 1971.

[12] St John DA, Poole AW, Sims I. Concrete petrography: a handbook of investigative techniques. London: Arnold; 1998.

[13] Gibbon GJ, Ballim Y, Grieve GRH. A low-cost, computer-controlled adiabatic calorimeter for determining the heat of hydration of concrete. ASTM J Test Evaluat 1997;25(2):261–6.

[14] Wang Ch, Dilger WH. Prediction of temperature distribution in hardening concrete. In: Springenschmid R, editor. Thermal cracking in concrete at early ages. London: E&FN Spon; 1994. p. 21–8.

[15] Naik TR. Maturity functions for concrete during winter conditions. In: Naik TR, editor. Temperature Effects on Concrete.

ASTM STP 858. Philadelphia: American Society for Testing and Materials; 1985.

[16] Bamford CH, Tipper CFH, editors. Comprehensive chemical kinetics Vol 1: The practice of kinetics. London: Elsevier Publishing Company; 1969.

[17] Ballim Y, Graham PC. A maturity approach to the rate of heat evolution in concrete. Magazine of Concrete Research 2003;55(3): 249–256.

[18] Broda M, Wirquin E, Duthoit B. Conception of an isothermal calorimeter for concrete—determination of the apparent activation energy. Mater Struct 2002;35:389–94.

[19] Xiong X, van Breugel K. Isothermal calorimetry study of blended cements and its application in numerical simulations. Heron 2001;46(3):151–9.

[20] Lawrence CD. The constitution and specification of Portland cements. In: Hewlett PC, editor. Lea's chemistry of cement and concrete. 4th ed. London: Arnold; 1988 [Chapter 4].

[21] Taylor HFW. Cement chemistry. 2nd ed. London: Thomas Telford; 1997.

[22] Addis BJ. Cementitious materials. In: Addis BJ, editor. Fulton's concrete technology. Midrand, South Africa: Cement and Concrete Institute; 2001 [Chapter 1].

[23] Lerch W. The influence of gypsum on the hydration and properties of Portland cement pastes. Proc ASTM—technical papers 1946;46:1252–97.

[24] Macphee DE, Lachowski EE. Cement components and their phase relations. In: Hewlett PC, editor. Lea's chemistry of cement and concrete. 4th ed. Arnold: London; 1988 [Chapter 3].

[25] Jackson PJ. Portland cement: classification and manufacture. In: Hewlett PC, editor. Lea's chemistry of cement and concrete. 4th ed. Arnold: London; 1988 [Chapter 2].

[26] Roode-Gutzmer QI, Ballim Y. Phase composition and quantitative X-ray powder diffraction analysis of Portland cement and clinker. In: Mindess S, Skalny J, editors. Materials science of concrete VI. American Ceramic Society; 2001 [Chapter 1].

[27] Maekawa K, Chaube R, Kishi T. Modelling concrete performance—hydration, microstructure formation and mass transport. London: E&FN Spon; 1999.

[28] Ballim Y. A low-cost heat model and calorimeter to predict temperature profiles in mass concrete elements. In: Proceedings of the 1st International Conference on Concrete and Development. Building and Housing Research Centre. Tehran, Iran, May 2001.